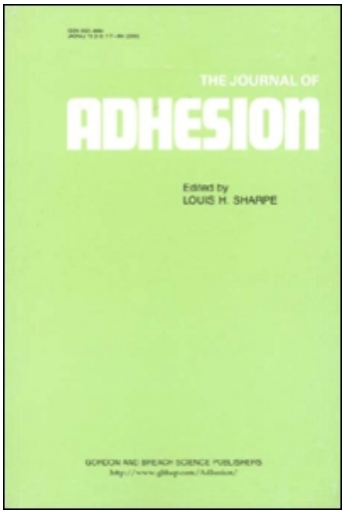

The Journal of Adhesion
Publication details, including instructions for authors and subscription information:
http://www.informaworld.com/smpp/title~content=t713453635

Application of Adhesion Model for Developing Hot Melt Adhesives Bonded to Polyolefin Surfaces

M. F. Tse[a]
[a] Polymer Science Division, Baytown Polymers Center, Exxon Chemical Company, Baytown, Texas, USA

To cite this Article Tse, M. F.(1995) 'Application of Adhesion Model for Developing Hot Melt Adhesives Bonded to Polyolefin Surfaces', The Journal of Adhesion, 48: 1, 149 — 167
To link to this Article: DOI: 10.1080/00218469508028160
URL: http://dx.doi.org/10.1080/00218469508028160

J. Adhesion, 1995, Vol. 48, pp. 149–167
Reprints available directly from the publisher
Photocopying permitted by license only

Application of Adhesion Model for Developing Hot Melt Adhesives Bonded to Polyolefin Surfaces*

M. F. TSE

Polymer Science Division, Baytown Polymers Center, Exxon Chemical Company, Baytown, Texas 77522, USA

(Received March 11, 1994; in final form July 20, 1994)

We have found that the adhesive strength, P, of hot melt adhesives (HMAs) based on semi-crystalline polymers can be described by the following equation:[1]

$$P = P_0BD \tag{1}$$

previously derived for tack of pressure sensitive adhesives (PSAs).[2,3] In this equation, P_0 is the interfacial adhesion between the adhesive and the substrate, B is the bonding term, and D is the debonding term. This adhesion model is then applied to the development of HMA formulations based on Exxon Chemical's olefinic polymers and Escorez® tackifiers, bonded to Escorene® polypropylene and polyethylene substrate surfaces. Two olefinic polymers, Escorene® EVA polymer (ethylene/vinyl acetate copolymer) and Exact™ polymer, will be used. EVA polymer is the industrial leader in HMA applications, whereas Exact™ polymer is a new family of linear ethylene copolymer products made using a new class of proprietary catalysts. Therefore, performance of HMAs based on EVA polymer and Exact™ polymer is compared in the context of the P_0, B, and D terms of our adhesion model. The interfacial adhesion P_0 term of these HMAs is generally governed by the surface tensions of the three HMA components: polymer, tackifier and wax. The bonding term, B, depends on the bonding temperature exponentially, and increases with the bonding time to a power of 1/6-1/2 at short bonding time. During the HMA bonding process, the low melt viscosity of the HMA facilitates sufficient spreading on a microscopically rough substrate surface. Therefore, the bonding term B is independent of the bonding pressure. The debonding term, D, depends on adhesive bulk properties. It is related to viscoelastic loss tangent in the industrial peel frequency range when the HMA/substrate assembly exhibits an apparent interfacial failure (AIF) mode, but to the tensile draw ratio at break of the bulk adhesive when the HMA/substrate assembly exhibits a mixed cohesive/apparent interfacial failure (CF/AIF) mode. Overall, compared with HMAs based on EVA polymers, HMAs based on Exact™ polymers show higher viscosity and inferior tensile strength, but better bond strength to polyolefin surfaces, higher strain at break, and lower yield stress.

KEY WORDS adhesion model; hot melt adhesive; polyolefin substrate; tackifier; surface tension; interdiffusion; loss tangent; polymers

1. INTRODUCTION

A. Hot Melt Adhesives

HMAs are usually formulated from a semi-crystalline polymer, a tackifier and a wax. They are compounded and applied in the molten state at elevated temperatures. The

* Previously presented at the International Symposium on Hot Melts (Port Jerome, France, November 8, 1993).

resultant properties are obtained when the adhesive is cooled to a tough and flexible solid to form the bond with the substrate surface. The polymer provides filmability, strength, flexibility and high temperature resistance. The tackifier contributes specific adhesion and surface wetting characteristics during the bonding process. The wax functions as a hot melt solvent to lower viscosity, alters HMA surface characteristics and controls adhesive set time/open time.

B. Adhesion Models

The design of adhesive systems has been practiced as an art rather than as a science for many years. However, about a couple decades ago, Gent and coworkers[4-7] began their efforts to examine the factors contributing to the strength of an adhesive bond. They proposed that the bond strength for the interface of a crosslinked, rubbery adhesive and a rigid substrate can be expressed by the following equation:

$$P = P_0 F \tag{2}$$

In the above equation, P_0 is the interfacial (or intrinsic) adhesion (attractive forces at adhesive/substrate interface: van der Waals, electrostatic, hydrogen bonding, acid-base, covalent chemical bonding and others). F is a rheological loss function of the bulk adhesive which depends strongly on rate and temperature. Essentially, F measures the energy dissipated in viscoelastic and plastic deformations at the crack tip (peel front). The physical significance of Eqs. (1) and (2) is that material around the crack tip of the adhesive joint can be subjected to a stress and strain environment for dissipating input mechanical energy, while the interfacial bonds (surface anchoring such as chemical bonds, physical bonds, or other intrinsic forces) acting ahead of the crack tip remain unbroken. Also, when the viscoelastic and plastic energy losses are negligible (such as the case of a very brittle adhesive), F will be approaching unity, and the measured bond strength, P, is equal to the intrinsic adhesion, P_0. Despite the physical soundness of Eq. (2), these researchers did not disclose the exact functional form of F.

By studying the joint strength of a model elastomer/treated aluminum assembly, Carre and Schultz[8] proposed a model with the energy of separation described by the product of three terms: the reversible energy of adhesion or cohesion, P_0, a molecular dissipation factor related to the degree of crosslinking of the elastomer, $g(M_c)$, and a macroscopic dissipation factor due to viscoelastic losses, F:

$$P = P_0 g(M_c) F \tag{3}$$

This approach allowed them to explain the widely-different bond strengths observed for various surface treatments of the metal substrate. They attributed these large differences to the various degrees of crosslinking of the elastomer in the vicinity of the interface, the degree of crosslinking being higher near the interface than in the bulk. When peel is performed under near-equilibrium conditions (low rate of separation and/or high temperature), F will approach unity and $P = P_0 g(M_c)$. Therefore, they equated $P_0 g(M_c)$ to the threshold value of energy of separation when measured at equilibrium. Again, similar to the studies of Gent and coworkers,[4-7] they did not describe the explicit form of F.

For organic adhesives on common polymeric substrates, the interfacial adhesion is typically of the order of 0.1 J/m^2 (6×10^{-4} lb/in). This could be deduced from the fact that the sum of surface tensions of most polymeric adhesives and substrates is in the range of 50–100 mJ/m^2 = 0.05-0.1 J/m^2. However, due to rheological energy dissipation in the crack tip, most practical measures of joint strength yield separation energies of 10^2–10^4 J/m^2 (0.6–60 lb/in), which are several orders of magnitude larger than the interfacial adhesion. Therefore, an explicit form of F is very important in the practice of adhesion science and technology. By recognizing this need, we[2,3] hypothesized that the pressure sensitive tack of the block copolymeric PSA/stainless steel interface can be described by Eq. (1).

For the sake of illustration, we consider a T-peel specimen of an adhesive bonded between two pieces of a substrate. The adhesive test method in which two strips of an adhesive joint are peeled apart symmetrically, at 180° in opposite directions, is referred to as "T-peeling". If we assume that the separated substrates are not elongated significantly (less than about 10%) under the peel force, F, the adhesive fracture energy is given by

$$G_a = 2F/w = 2P \tag{4}$$

where w is the width of the bonded strips, and P is the peel strength. The peel strength, P, consists of two terms:

$$P = P_0B + P_0BD' = P_0BD \tag{1}$$

The first term is the debonding energy to overcome surface anchoring. This term is normally very small, and is the product of the interfacial adhesion, P_0, and the bonding term, B. The second term is the energy dissipation in the adhesive, which is usually large, expressed by the product of P_0, B, and D'. D' can be considered as an energy dissipation term. Energy dissipation is the amount of energy absorbed by the bulk adhesive to keep this energy from being transferred to the interface to break the interfacial bond. In other words, it functions like a shock absorber or an energy sink. After a simple rearrangement, the last equation can be transformed back to Eq. (1), if $D \equiv 1 + D'$.

For block copolymeric PSA/stainless steel assemblies, we have found that, when the PSAs fulfill the Dahlquist criterion,[9] B = constant, and the debonding function, D, can be represented by

$$D = K_1 \log G''(a_T\omega) + K_2 \tag{1a}$$

where K_1 and K_2 are constants, and G'' is the loss modulus of the bulk adhesive at the reduced frequency $a_T\omega$ corresponding to the separation speed of the particular PSA test.[2,3] We believe that Eq. (1) is general and could be applied to other PSAs, such as those based on emulsion acrylics and radiation-cured polymers. Yang[10] deduced the following relationships for emulsion acrylic PSA data:

$$B \sim 1/G' \tag{1b}$$

and

$$D \sim (C_1G'' + C_2) \tag{1c}$$

for fitting Eq. (1). The G' value was determined at PSA bonding frequency, 1 s^{-1}, proposed by Dahlquist.[9] The G'' value was determined at PSA debonding frequency.[2,3]

C. Adhesive Bond Formation

Voyutskii[11] and Vasenin[12] proposed that autohesion and adhesion of polymers are due to mutual diffusion of polymer molecules across the interface. By assuming that bond strength is proportional to the product of number of molecules intersecting the interface and the depth of penetration (the latter being obtained by applying the proper boundary conditions to Fick's second law), they arrived at the following expression for adhesive fracture energy:

$$G_a \sim t^{1/4} \tag{5}$$

where t is the contact time.

Kausch *et al.*[13] in Lausanne, Switzerland, performed compact tension tests on re-healed and welded glassy polymers (PMMA/PMMA, SAN/SAN, and PMMA/SAN). At temperatures above T_g, fracture energy per unit area at the interface increased with contact time in the form:

$$G_a \sim t^{1/2} \tag{6}$$

Both de Gennes[14] and Wool,[15] using somewhat different arguments, derived the above expression theoretically based on the reptation model of chain dynamics.[16]

Recently, de Gennes[17] derived the following expression for G_a of an adhesive joint formed by contacting two slightly incompatible polymers 1 and 2:

$$G_a \sim (RT/N_a)^{1/2} \exp[-N_e \alpha^3 (\Delta\delta)^2 N_a/RT] \tag{7}$$

where R is the gas constant, T is the temperature, N_a is Avogadro's number, N_e is the number of monomers in an entanglement chain, α is the size of a polymer repeat unit, and $\Delta\delta$ is the solubility parameter difference between polymers 1 and 2 as described by the Hildebrand-Scott relation:[18]

$$\chi = \text{Flory interaction parameter} = [\alpha^3 (\Delta\delta)^2/kT] \tag{8}$$

The Flory interaction parameter is the energy required for a repeat unit of polymer 1 to diffuse into polymer 2 divided by kT, where k is the Boltzmann's constant. His assumptions are: (1) N_e is of similar magnitude for polymers 1 and 2, (2) $\chi \ll 1$ so that the interface is diffuse, and (3) adhesive joint formation between 1 and 2 requires some portion of the chains in polymer 2, for example, to have a length at the interface larger than αN_e.

Also, the interfacial thickness, I, can be described by:

$$I = \alpha \chi^{-1/2} \tag{9}$$

II EXPERIMENTAL

A. Materials

Figure 1 is a brief introduction of the polymers, the tackifiers, and the wax used in this study. The EVA polymer has a vinyl acetate content of 28 wt. %, and a melt index of 32. The Exact™ polymer, which has a melt index of 31, is a linear ethylene copolymer

POLYMERS

Escorene ® 7750: Ethylene/Vinyl Acetate Copolymer (28 Wt.% Vinyl Acetate; MI = 32); Exxon Chemical
Exact™ Polymer: MI = 31; Exxon Chemical

TACKIFIERS

Hydrocarbon Tackifiers

- **Feeds From Petroleum Sources; Lewis Acid Or Thermal Polymerization**

Tackifier (Exxon Chemical)	*Type*	*GPC M_w*	*DSC T_g, °C*
Escorez® 1310LC	Aliphatic	1460	46
Escorez ® 2393	Aliphatic-Aromatic	995	45
ECR-327	Hydrogenated Cyclic	340	-13

Rosin Derivatives

- **Mixtures Of Abietic Acids Modified Via Disproportionation, Polymerization, Hydrogenation, Or Esterification**

Rosin Ester: M_n = 810, M_w = 970; DSC T_g = 53°C

Wax

Petroleum Wax: Aristowax® 165; M_n = 410, M_w = 460; DSC T_m = 68°C

FIGURE 1 Description of polymers, tackifiers, and wax.

made using Exxon Chemical's new class of proprietary catalysts. It has a narrow composition distribution and a narrow molecular weight distribution.

Escorez® hydrocarbon tackifiers are cationic or thermally polymerized from monomer feeds obtained from petroleum sources. Figure 1 shows some tackifiers used in this study. M_w is the weight average molecular weight determined by GPC. T_g is the glass transition temperature determined by DSC.

The other type of tackifier is based on rosin acid obtained from pine trees. Various chemical methods are used to modify rosin acid to make it more stable and non-crystallized. One example is a rosin ester obtained by reacting a multi-functional alcohol with the rosin acid. The product used in this study has a M_n of 810, M_w of 970, and a DSC T_g of 53°C.

Only one type of wax, Aristowax® 165, was used in this study. It has a M_n of 410, M_w of 460, and a DSC melting point, T_m, of 68°C.

B. Surface Tension Measurements

A pendant drop tensiometer, which was designed by Koberstein at University of Connecticut, was used to measure surface tensions of the HMA components. It involves determining the shape of a fluid drop which hangs from the bottom of a vertical capillary tube in air. The drop profile is governed by the force balance between gravity pulling the fluid down (ρg = gravitational force per unit fluid volume) and the fluid/air interfacial tension (γ) holding the drop in place:

$$\gamma/a^2 = (\rho g)/B^2$$

where a = radius of curvature at drop apex, ρ = fluid density, g = gravitational constant and B^2 = shape factor.

C. Specimen Preparation, Viscoelastic and Stress-Strain Measurements

Three different formulations were used, as shown in Figure 2. Each adhesive blend was prepared by hot melt blending. A simple description of the polypropylene (PP), polyethylene (PE) and aluminum (Al) substrates was also given.

For the preparation of the T-peel specimens, a thin sheet of adhesive sample was laminated between two pieces of the substrate in a positive pressure, Teflon-coated mold. Adhesive thickness, t_a, was controlled at 6 mils = 152 μm. The laminate was then cut into 1/2″ = 1.3 cm wide specimens. All the T-peel measurements were done at a separation speed of v = 2″/min = 847 μm/s.

Therefore, the adhesive in the vicinity of the separation zone could experience an approximate debonding frequency, f, (expressed in s^{-1}):[2,3]

$$f = v/2t_a \tag{10}$$

Under the above conditions, f = 2.8 Hz.

Specimens for viscoelastic and tensile stress-strain studies were made by compression-molding the adhesive material between Teflon-coated aluminum foil. Isothermal dynamic mechanical experiments were performed using the Polymer Laboratories DMTA over a wide range of temperatures. For tensile stress-strain measurements, the molded samples were die-cut into micro-dumbbell specimens (ASTM D1708). A crosshead speed of 2″/min = 847 μm/s was used. The stress was calculated based on the undeformed cross-sectional area of the tensile specimens.

ADHESIVES (Ingredients In Parts By Weight)

	HMA 1	HMA 2	HMA 3
Escorene® 7750	45	45	–
Exact™ Polymer	–	–	45
Escorez® 1310LC	–	–	22
Escorez® 2393	45	–	–
ECR-327	–	–	33
Rosin Ester	–	45	–
Aristowax® 165	10	10	–
Irganox® 1010	0.5	0.5	0.5

SUBSTRATES

PP: Escorene® 4252; M_n = 80K, M_w = 297K; DSC T_m = 163°C; Thickness = 130 μm; Exxon Chemical

PE: Escorene® LD-117.08; MI = 1.5-2.0; Density = 0.93 g/cm³; Thickness = 130 μm; Exxon Chemical

Al: Reynolds® 667; Shiny Side For HMA Bonding; Thickness = 20 μm; Reynolds Metals

FIGURE 2 Adhesive formulations and substrates used in this work.

III RESULTS AND DISCUSSION

A. HMA Interfacial Adhesion

According to thermodynamics, P_0 can be written as follows:

$$P_0 \sim \gamma_a + \gamma_s - \gamma_{as}$$

where γ_a = surface tension of the adhesive, γ_s = surface tension of the substrate, and γ_{as} = interfacial tension between the adhesive and the substrate. This interfacial adhesion term, P_0, although small in magnitude, could influence P strongly due to the multiplicative nature of Eq. (1).

A simple rule to design an adhesive for bonding a given substrate is by comparing the values of γ_a and γ_s. If the adhesive has a higher surface tension than the substrate, wetting is less likely to occur. On the other hand, if the adhesive has a lower surface tension than the substrate, wetting will occur more readily.

Figure 3 shows the surface tension as a function of temperature for the various HMA components determined by the pendant drop method. The magnitude of surface tension in decreasing order is: EVA, rosin ester, ECR-327, PE, Escorez 2393, Escorez 1310LC, PP and paraffin wax. Therefore, when we blend tackifier and wax with EVA, according to thermodynamics, the lower surface tension and lower molecular weight wax or tackifier may bloom to the EVA surface.

All these surface tensions were measured in the molten state. The data of surface tension *versus* temperature T for each material obeys a linear relation described by the following equation:

$$\gamma = -(d\gamma/dT)T + \text{Constant}$$

A simple guiding hypothesis for optimizing the interfacial adhesion term, P_0, of the adhesive/substrate system is shown in Figure 4. The P_0 term should be highly

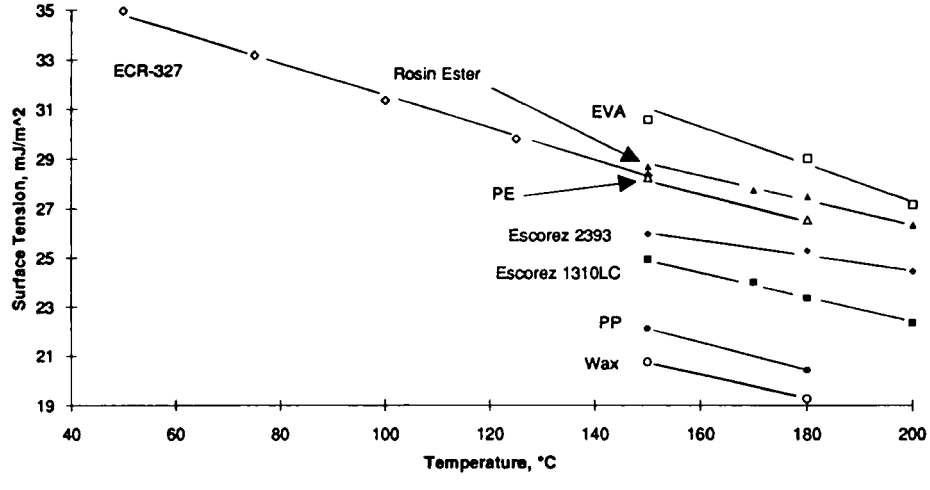

FIGURE 3 Surface tension *versus* temperature of HMA components measured by pendant drop method.

Polymer	Tackifier	Surface Of Polymer/ Tackifier Blend	Surface Of Substrate	P_o	Example
P	P	P	P	High	EVA/RE to Al
N-P	N-P	N-P	N-P	High	Ex/Es to PP
P	N-P	N-P	N-P	Medium	EVA/Es to PP
P	P	P	N-P	Low	EVA/RE to PP
N-P	N-P	N-P	P	Low	Ex/Es to Al

Es: Escorez® Tackifier Ex: Exact™ Polymer PP: Polypropylene
EVA: Escorene® 7750 RE: Rosin Ester Al: Aluminum

FIGURE 4 A guiding hypothesis for optimizing interfacial adhesion.

dependent on the polar/non-polar nature of the HMA and the substrate. We have shown in a previous study[1] that the surface of the EVA/Escorez® tackifier blend is enriched in tackifier, which, in this case, is non-polar, and of low molecular weight and low surface tension compared with the EVA polymer. For the Exact™ polymer/rosin ester blend, we speculate that the surface of the blend is enriched in polymer due to the non-polar nature of this polymer.

B. HMA Bonding Process

1 Effects of Bonding Temperature We quantify the bonding term B in Eq. (1) by studying the effects of bonding temperature, T_b, on peel strength in Figure 5. Bonding time and bonding pressure were kept at 10 s and 40 psi (0.28 MPa), respectively. For HMA 2 bonded to PP, peel strength behaved differently in three different bonding temperature regions: 100–140°C, 140–170°C and above 170°C. In the low bonding temperature region, adhesion increased rather slowly, and the HMA exhibited a slip-stick AIF mode. In the intermediate bonding temperature region, adhesion increased quite sharply (melting point of the PP substrate is 163°C according to DSC) and the HMA exhibited an AIF mode. In the high bonding temperature region with a single data point, adhesion decreased slightly and the adhesive exhibited a mixed CF/AIF mode. Similar behavior was observed for HMA 1 bonded to PP.

Bonding temperature effects on peel strength of HMA 3 to both PP and PE substrates are also shown in Figure 5. These HMA/polyolefin assemblies exhibited AIF mode without any slip-stick motion.

Without the consideration of the last data point at 180°C for HMA 2 in Figure 5, the peel strength of each HMA/polyolefin substrate system appears to obey the Arrhenius behavior:

$$P \sim \exp(-E_d/RT_b) \tag{11}$$

where R is the gas constant, and E_d is a certain type of activation energy which will be discussed in detail in a later part of this section.

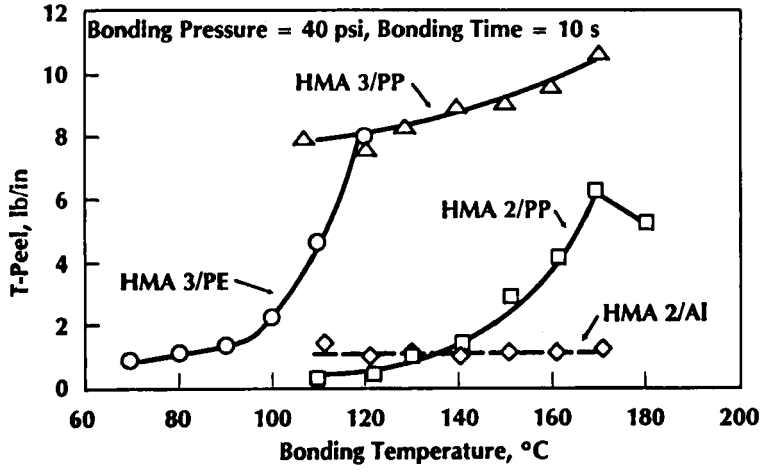

- Peel Strength ~ Exp ($-E_d/RT_b$), R = Gas Constant

HMA	Substrate	E_d, kcal/mole	E_η, kcal/mole
1	PP	20.8	11.6
2	PP	12.8	11.7
3	PE	10.8	9.72
3	PP	1.58	9.72

E_η = Activation Energy For Flow; E_d = Activation Energy For Interdiffusion?

- Peel Strength ~ Constant For HMA Adhered To Immiscible Aluminum Surface

FIGURE 5 Changes in peel strength with bonding temperature for HMAs 2 and 3; PP and Al substrates, bonding time = 10 s and bonding pressure = 40 psi (0.28 MPa).

An expression such as Eq. (11) may lead one to think that HMA bond strength would be controlled by wetting flow of the adhesives if E_d had a value similar to E_η, activation energy of flow of the HMA. However, according to the table shown in Figure 5, E_η's of these HMAs obtained by rheological measurements (Figure 6; zero shear viscosity ~ $\exp(E_\eta/RT)$) are not exactly identical to E_d. This is not surprising because molten HMAs should have good wetting with the substrate surface due to their low viscosities at elevated temperatures. Therefore, E_d should represent activation energy of a bonding mechanism other than the wetting flow process of the molten HMA. As shown in Figure 6, HMAs based on Escorene® EVA polymer have lower melt viscosities than the HMA based on Exact™ polymer. Upon dilution by tackifier (hot melt solvent), branched EVA is less viscous than linear Exact™ polymer due to a smaller molecular size.

Another piece of experimental evidence opposing the wetting flow mechanism is described as follows. We bonded HMA 2 to the aluminum (Al) substrate at various bonding temperatures, under the same bonding conditions of 40 psi (0.28 MPa) and 10 s. The Al substrate is assumed to be totally immiscible with the adhesive. Therefore, HMA/Al interactions are limited to surface sites. These results compared with those of the same HMA bonded to PP are also shown in Figure 5. It appears that at, or above,

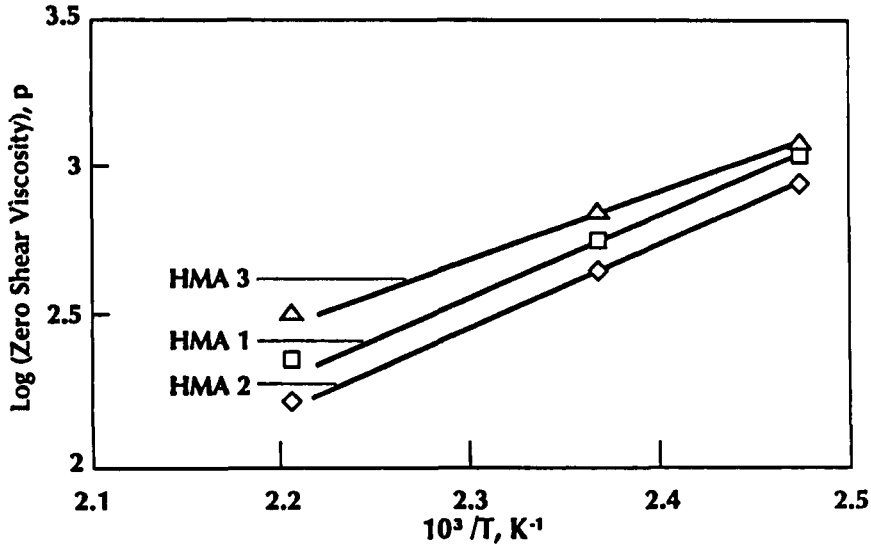

FIGURE 6 Activation energy of flow determined from temperature dependence of zero shear viscosity.

110°C the HMA viscosity is low enough so that the bulk adhesive flows readily into and around the surface features of the immiscible substrate. This will result in peel strength independent of the application temperature of the adhesive.

Without direct evidence, we suspect that E_d may describe a certain type of limited interdiffusion between HMA and PP substrate during the bonding process. Especially for HMAs 1 and 2 bonded to PP, the sharp transition from low to high bond strength, plus the change in failure mode when the bonding temperature approaches T_m of the PP substrate (Figure 5), could suggest an interdiffused layer formed at the HMA/PP interface at higher bonding temperatures. There may be some specific interactions, such as association or neutralization, between EVA and rosin ester in HMA 2. These may enhance chain diffusion to a limited degree into PP, resulting in a lower E_d compared with that of HMA 1. Of course, the lower E_d values for HMA 3/polyolefin substrate systems could indicate a greater degree of compatibility between adhesive and substrate during HMA bonding. Limited interdiffusion of these systems could occur more readily than for the EVA HMA/polyolefin substrate systems.

To understand further the dependence of peel strength on HMA/polyolefin substrate compatibility, we rewrite Eq. (7) in the following form:

$$P = A(RT_b)^{1/2} \exp(-B/RT_b)$$

where A is a constant and $B = N_e \alpha^3 (\Delta\delta)^2 N_a$. Using A and B as the two adjustable parameters, we arrive at the solid curves in Figure 7 which are the best fit of the experimental data to the last equation. These A and B values are also shown in Figure 7.

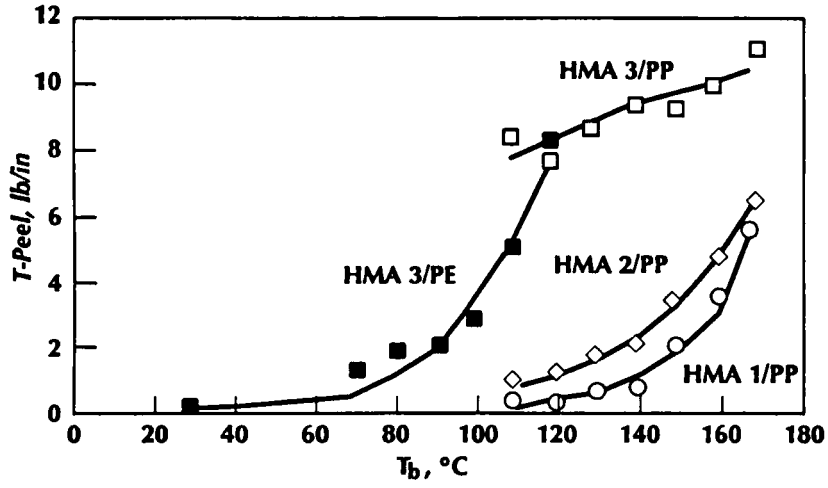

HMA	Substrate	A, (mole/l)$^{1/2}$lb/in	B, J/mole
1	pp	664	11923
2	PP	15.23	6398
3	PE	13.52	4009
3	PP	0.31	185

FIGURE 7 Solid curves are best fit to the equation derived by de Gennes (Ref. 17) for the experimental data of the four HMA/polyolefin substrate systems.

As shown in Figure 8, we used literature values of entanglement molecular weights[19,20] of 1250, 6900, and 3550 for polyethylene, poly(vinyl acetate) and 1,2-polybutadiene [an approximation for poly(butene-1)], respectively. We also used the characteristic ratios (C_∞'s) of the various homopolymer structures[21] and the equation: $\alpha = (2C_\infty)^{1/2}(1.54\,\text{Å})$ for vinyl polymers to calculate the sizes of polymer repeat unit [5.32 Å and 5.13 Å for the EVA and Exact^{TM} polymers, respectively]. In choosing the C_∞ value for a given polymer structure, we picked the one with the minimum value to simulate a θ-solvent or melt condition [5.3 for polyethylene, 7.9 for poly (vinyl acetate) and 6.6 for poly(butene-1)]. With the assumption of tackifier(s) or tackifier/wax blend as a hot melt solvent for the polymer during the bonding process, we determined the values of $\Delta\delta$ from the values of B for the different HMA/polyolefin substrate systems shown in the table of Figure 8. This figure also shows the plot of peel strength data at bonding temperatures of 120 and 160°C for the HMA/PE and HMA/PP systems, respectively, *versus* these $\Delta\delta$ values. We selected these peel strength values at bonding temperatures (120 and 160°C) close to the melting temperatures of the two polyolefin substrates, *PE* and *PP*. This plot clearly indicates that adhesive bond strength drops with increasing HMA/substrate incompatibility.

We calculated the Flory interaction parameter, χ, and the interfacial thickness, I, from the $\Delta\delta$ values according to Eqs. (8) and (9), respectively. Similarly, temperatures of 120 and 160°C were used for the PE and PP substrates, respectively. The results are listed in the table of Figure 8.

$$B = N_e a^3 (\Delta\delta)^2 N_a$$

$$a = (2C_\infty)^{1/2}(1.54\ \text{Å})$$

$$\chi = \alpha^3(\Delta\delta)^2$$

$$l = \alpha\chi^{-1/2}$$

Where C_∞ = Characteristic Ratio

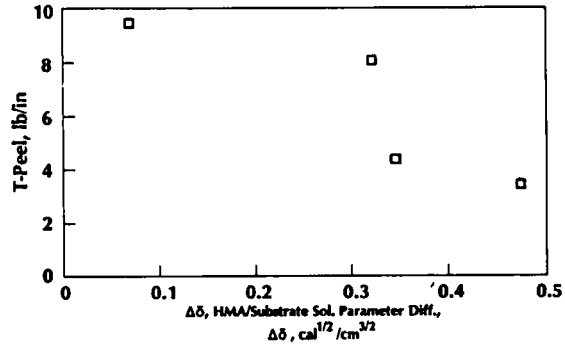

HMA	Substrate	T, °C	Δδ, $cal^{1/2}/cm^{3/2}$	$\chi \times 10^2$	l, Å
1	PP	160	0.47	2.33	35
2	PP	160	0.34	1.25	48
3	PE	120	0.32	1.06	50
3	PP	160	0.07	0.044	240

- **More Compatible HMA/Substrate System, Signified By Smaller Δ δ, Has Smaller χ, Larger l, And Higher Peel Strength**

FIGURE 8 Thermodynamic and interfacial parameters for HMA/polyolefin interface.

Smaller solubility parameter difference or Flory interaction parameter, χ, means better HMA/polyolefin substrate compatibility, hence larger interfacial thickness. If the interactions are mainly van der Waals attractions, then χ is positive. The case $\chi = 0$ corresponds to a HMA with chemical nature very similar to the substrate and the above analysis becomes invalid.

In summary, HMA bonding kinetics differs as compatibility between HMA and polyolefin substrate changes. Several basic thermodynamic and interfacial parameters could be deduced from these experimental peel strength/bonding temperature relations.

2 *Effects of Bonding Time* Our next step to quantify B is to examine the effects of bonding time, t_b on peel strength. We focused on HMAs 2 and 3 bonded to PP. The behavior of HMA 2 (at three different bonding temperatures: 130, 150, and 170°C) and HMA 3 (at a single bonding temperature: 150°C) is shown in Figure 9. If we assume that PP has a thermal diffusivity of $1.6 \times 10^{-3}\,cm^2/s$, we can calculate that the time for complete heat conduction through the 130 μm PP substrate is 0.3 s.[22] The shortest bonding time used was 1 s in Figure 9. Therefore, heat transfer to HMA should be complete.

For HMA 2, if we disregard the bonding temperature effects due to the large scatter of data points, peel strength appears to increase steadily with bonding time for bonding times < 10 s. It then levels off to a plateau or drops very slightly at longer bonding times. At long bonding times, the HMA/PP assembly appears to have similar bond strength independent of the bonding temperature used. Usually the HMA exhibited slip-stick AIF mode at short bonding times as the peel strength was still increasing, but

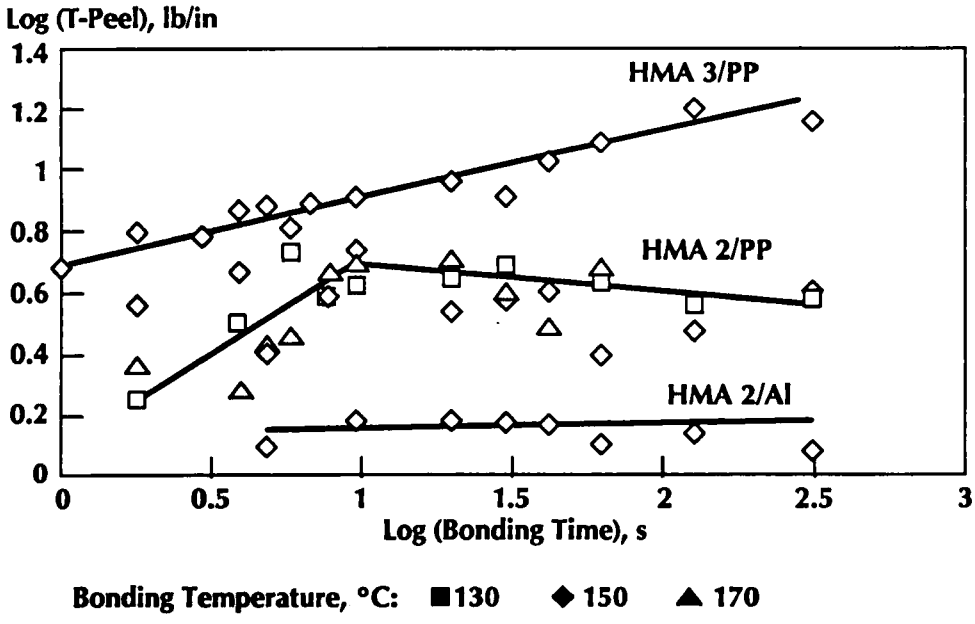

FIGURE 9 Effects of bonding time on peel strength with PP and Al; bonding pressure = 40 psi (0.28 MPa); various bonding temperatures.

it exhibited AIF mode at long bonding times as the peel strength stayed approximately constant.

The peel strength of HMA 3 showed different behavior. It continued to increase up to a bonding time of 300 s. This behavior is consistent with the low $\Delta\delta$ of the HMA 3/PP system described in Figure 8. The adhesive exhibited AIF mode except at the two longest bonding times: 120 and 300 s. In the latter two cases, the adhesive exhibited mixed CF/AIF mode.

To gain kinetic information for the HMA 2/PP system, we focus on the peel strength data shown in Figure 9 at short bonding times. These experimental data can be represented by the following equation:

$$P = (t_b/t_0)^{0.42} = (t_b/0.24)^{0.42}, \text{ correlation coefficient} = 0.6267$$

where $t_0 = 0.24$ s is the response or induction time for the bond to reach a peel strength of 1 lb/in (0.18 kg/cm). The correlation is poor but it provides some scientific insight into the bonding process. Because the exponent in the last equation is intermediate between 1/4 and 1/2 (see Eqs (4)–(6)), we speculate that the HMA, a mixture of polymer (EVA) and oligomeric materials (tackifier and wax), may penetrate into the PP substrate, to a limited degree, by combined reptation/Fickian diffusion.

For the HMA 3/PP system, we have somewhat different behavior:

$$P = (t_b/t_o)^{0.19} = (t_b/0.00013)^{0.19}, \text{ correlation coefficient} = 0.9600$$

The exponent is slightly larger than 1/6 but smaller than 1/4. Therefore, this behavior cannot be explained by both Eqs. (5) and (6).

By combining the results of this section and Eq. (11) for HMAs bonded to PP, the bonding term in our adhesion model could be described by

$$B \sim \exp(-E_d/RT_b)(t_b/t_0)^m, \quad 1/6 < m < 1/2 \tag{12}$$

We also stressed in Section III.B.1 that, due to the difference between E_d and E_η, bond strength is not controlled by the wetting flow of the adhesive. In our case, molten HMAs should have good wetting with the substrate surface due to their low viscosities at elevated temperatures.

Similar to what we discussed in Section III.B.1, bonding experiments for the HMA 2 and Al assembly have been performed at a bonding temperature of 150°C for various bonding times. The results, shown in Figure 9, indicate that peel strength is independent of bonding time. Thus, contrary to Eq. (12), for bonding of the same HMA to an immiscible surface

$$B \sim \text{Constant} \tag{13}$$

at different bonding times and bonding temperatures. In other words, for the HMA/PP system, the adhering materials could be partially miscible with each other so that an interphase of interdiffused molecules is possibly formed between them. Again, without direct evidence, we suspect that E_d in Eq. (12) may represent the activation energy of interdiffusion between HMA and PP substrate.

3 Effects of Bonding Pressure Figure 10 shows the effects of bonding pressure p_b on peel strength of HMAs 1 and 2 bonded to PP at a bonding temperature of 150°C and a bonding time of 10 s. It appears that there is no, or a very minimal, increase in adhesive

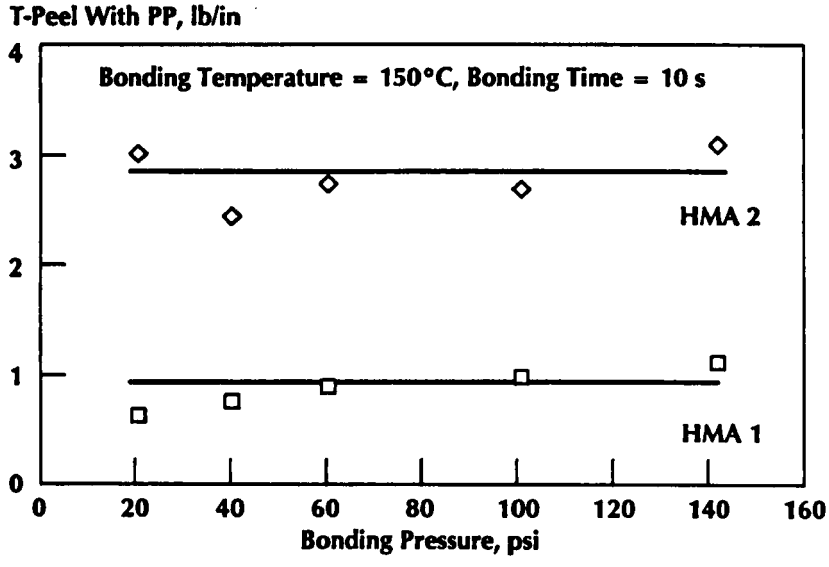

FIGURE 10 High bonding pressure is not required to enhance forced flow for HMAs with low melt viscosities.

strength with bonding pressure. These two HMAs have low enough viscosities at 150°C so that there is an appreciable amount of spreading on the microscopically-rough substrate surface. Therefore, higher bonding pressure is not required to enhance forced flow.

C. HMA Debonding Process

The adhesive and sealant industry has found that the EVA, Escorez® and wax system such as HMA 1 is good for bonding to paper but not so good to PP. Therefore, the peel strength of this adhesive to PP is quite low (Figure 11). The good bond strength of HMA 1 with paper is possibly due to high P_0 (mechanical interlocking). On the other hand, industry finds that, although the EVA, rosin ester and wax system such as HMA 2 has low P_0 (Figure 4), it performs better on PP, as shown by a higher energy dissipation and a higher peel strength. HMA 3 has high P_0 (Figure 4) and enhanced energy dissipation, hence improved peel test performance of the adhesive to PP. The peel strength is over 6 lb/in (1.1 kg/cm) *versus* 3 lb/in (0.54 kg/cm) for the industry EVA system.

Depending on the failure mode of the HMA/substrate system, the debonding term, D, represented by the energy dissipation in the bulk adhesive, can be measured either by viscoelastic loss tangent (small strain experiment) or by tensile draw ratio at break (large strain experiment) as detailed later. Draw ratio at break is defined as [1 + strain at break].

Figure 11 also shows the stress-strain curves of HMAs 2 and 3. Overall, compared with HMAs based on EVA polymer, HMAs based on Exact™ polymer show higher

Adhesive	Substrate	P_0	D	Peel Strength, lb/in
HMA 1 (N-P)	N-P	Medium	Low	1.7
HMA 2 (P)	N-P	Low	High	3.3
HMA 3 (N-P)	N-P	High	High	6.3

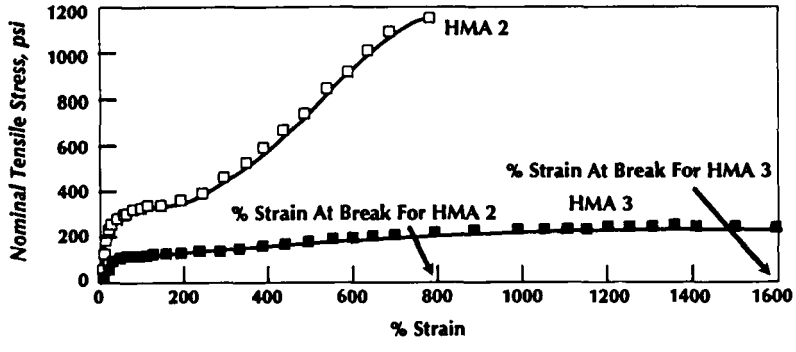

FIGURE 11 The role of energy dissipation, D, in HMAs bonded to polypropylene.

melt viscosity (Figure 6) and inferior tensile strength, but better bond strength to polyolefins (Figure 7), higher strain at break and lower yield stress.

One way to measure energy dissipation of the bulk adhesive is by using viscoelastic experiments (Figure 12). We placed the adhesive between two parallel plates and applied an oscillatory displacement to the material.[2,3] The frequency of oscillation was varied and the energy dissipation, represented by loss tangent [= (loss modulus)/(storage modulus)], was measured. We plotted the measured energy dissipation against frequency in Figure 12 for two adhesive systems: a good adhesive and a poor adhesive. Using Eq. (10), we calculated a frequency range, which corresponds to the separation speeds of the industrial test, as indicated by the two dotted lines. Within this frequency range, higher energy dissipation means stronger adhesion. Therefore, if energy dissipation is a measure of adhesion, it should be directly proportional to an attribute like peel strength.

One example is shown in Figure 13 for HMAs exhibiting AIF mode when peeled from PP substrate. We plotted peel strength *versus* loss tangent at T-peeling debonding frequency for a set of adhesives with similar amount of surface anchoring (similar interfacial adhesion term, P_0) and identical bonding conditions (identical bonding term, B). In this figure, the filled and empty squares represent the EVA HMAs and the HMAs formulated from Exact^{TM} polymers, respectively. Here, the data points represent HMAs formulated from EVA polymers and Exact^{TM} polymers of different melt indices. Also, some of these HMAs have formulations different from those shown in Figure 2. We have found in Figure 13 that, the higher the energy dissipation, the better

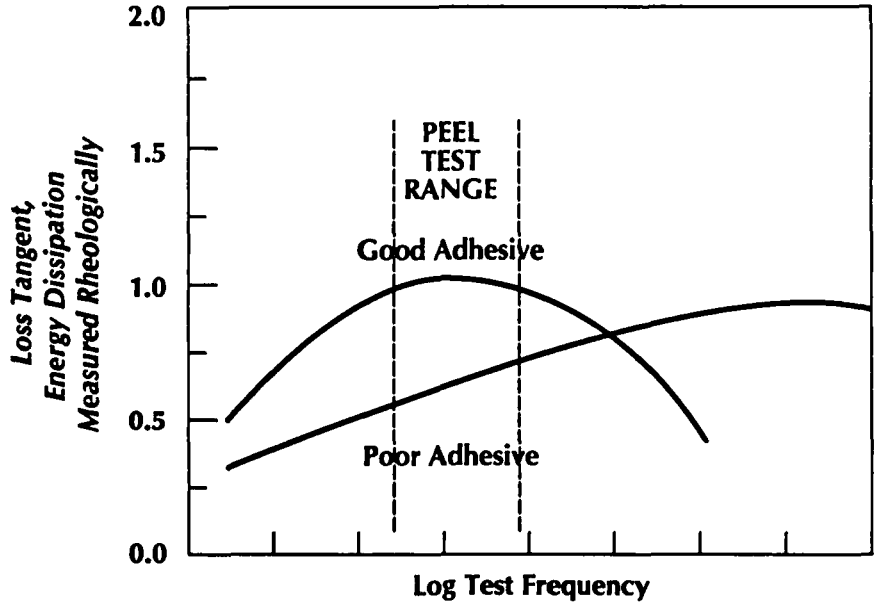

FIGURE 12 Peel test interpreted as adhesive energy dissipation at test frequency.

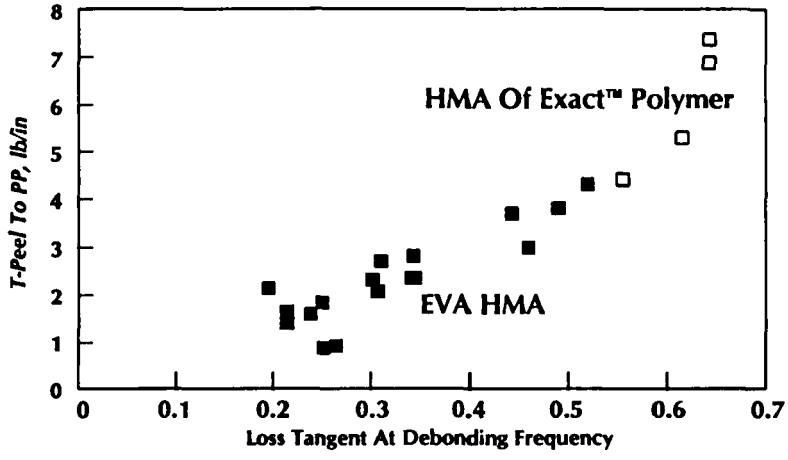

FIGURE 13 For HMA/PP bonds which exhibit AIF mode, bond strength increases with loss tangent of the bulk adhesive at T-peel debonding frequency.

is the peel adhesion as expressed by the following equation:

$$P \sim \tan\delta$$

Because $B =$ constant, and $P_0 \cong$ constant, we can convert the last equation to

$$D \sim \tan\delta \quad \text{(Failure Mode: AIF)}$$

by using Eq. (1). Overall, HMAs of Exact^{TM} polymers show higher values of loss tangent at debonding frequency than EVA HMAs, hence higher peel strength to PP.

On the other hand, Figure 14 shows that, if the failure mode of the HMA is CF/AIF, peel strength increases with adhesive draw ratio at break, λ_B, in accordance with:

$$P \sim \lambda_B$$

Again, the data points shown in Figure 14 represent HMAs formulated from EVA polymers and Exact^{TM} polymers of different melt indices. Also, some of these HMAs have formulations different from those shown in Figure 2. By using an argument identical to that described in the last paragraph, we can convert the last equation to

$$D \sim \lambda_B \quad \text{(Failure Mode: CF/AIF)}$$

Overall, HMAs of Exact^{TM} polymers show a higher degree of ductility than EVA HMAs, hence higher peel strength to PP.

In summary, the debonding term D of HMA ruptured in AIF mode appears to increase with the loss tangent at T-peel debonding frequency. On the other hand, debonding term D of HMA ruptured in CF/AIF mode appears to increase with the draw ratio at break of the adhesive.

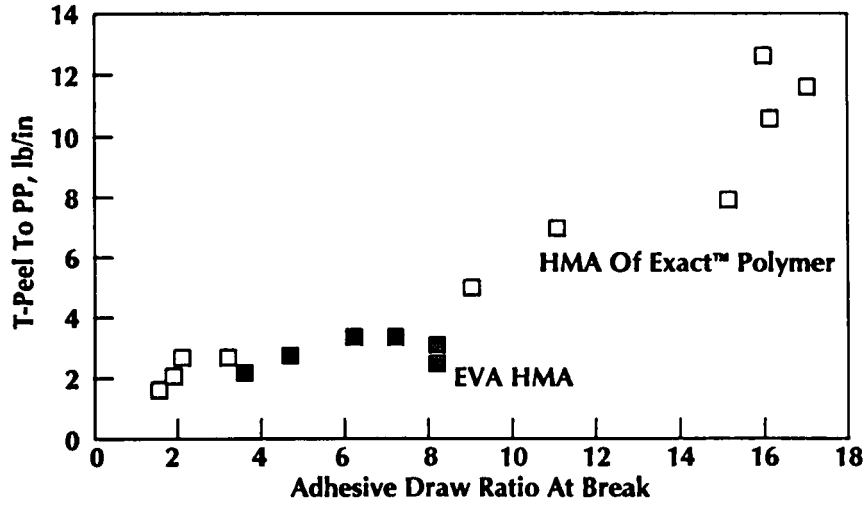

FIGURE 14 For HMA/PP bonds which exhibit AIF mode, bond strength increases with adhesive draw ratio at break.

IV CONCLUSIONS

The following table summarizes our findings:

HMA Predictive Model: $P = P_0 BD$

Adhesion Process	Controlling Factor	Functional Form
Intrinsic adhesion	Surface & interfacial tensions of HMA & substrate; WBL	$P_0 \sim W_a \sim \gamma_a + \gamma_s - \gamma_{as}$
Bonding	Bonding time/temperature/pressure, substrate physical structure	$B \sim [\exp(-E_d/RT_b)] \times [t_b/t_0)^m] (1/6 < m < 1/2)$; indep. of p_b
Debonding	Energy loss in HMA & substrate deformation	$D \sim \tan\delta$ (AIF) $D \sim \lambda_B$ (CF/AIF)

In the above table, we show that the interfacial adhesion P_0 is proportional to the thermodynamic work of adhesion, W_a, which is the sum of surface tensions of the adhesive and the substrate minus their interfacial tension, all quantities being measured at the bonding temperature. WBL stands for weak boundary layer.[1] The bonding term B depends on the bonding temperature T_b exponentially. From this experimental relationship, we could deduce the activation energy for limited interdiffusion, E_d. Furthermore, we could estimate several useful thermodynamic and interfacial parameters (solubility parameter difference $\Delta\delta$, Flory interaction parameter, χ, and interfacial thickness, I) of the HMA/polyolefin substrate systems based on an equation

derived by de Gennes.[17] The bonding term B also varies with the bonding time to the power m which has a value between 1/6 and 1/2, representing possibly different physical phenomena at the HMA/PP interface. Due to the very low melt viscosity of the HMA at bonding temperature, bonding pressure p_b (or forced flow) has no effects on strength of adhesion. The debonding term D depends on adhesive joint failure mode. D of HMA ruptured in AIF mode increases with the loss tangent of the adhesive at bond rupture frequency, tan δ. D of HMA ruptured in mixed CF/AIF mode increases with adhesive draw ratio at break, λ_B.

According to Eqs. (1a–c), (13) and the above table, Eq. (1) ($P = P_0 BD$) appears to be valid for PSAs, and HMAs based on semi-crystalline polymers. However, functional forms of B and D will depend on adhesive type, substrate type and the failure mode of the adhesive/substrate system.

V Acknowledgements

The author would like to thank P. Brant, M.D. Adamowicz, V.L. Hughes, P.-G. de Gennes and J.D. Domine for helpful discussion/communication, A.K. Mehta for supplying the Exact™ polymers, and D.W. Abmayr, Jr. for experimental assistance.

References

1. M. F. Tse, M. Faissat, *Proc. Eurocoat Conference*, Nice, France, September, 17, 1993.
2. M. F. Tse, *J. Adhesion Sci. Technol.*, **3(7)**, 551 (1989).
3. M. F. Tse, *Proc. European Tape & Label Conference*, Brussels, Belgium, April 29, 1993; *PSTC Annual Technical Seminar Proc.*, Tech XVI, Schaumburg, Illinois, USA, May 7, 1993.
4. A. N. Gent, A. J. Kinloch, *J. Polym. Sci.*, Part A-2 **9**, 659 (1971).
5. A. N. Gent, J. Schultz, *J. Adhesion* **3**, 281 (1972).
6. E. H. Andrews, A. J. Kinloch, *Proc. R. Soc. London*, Ser. A **322**, 385 (1973).
7. E. H. Andrews, A. J. Kinloch, *Proc. R. Soc. London*, Ser. A **322**, 401 (1973).
8. A. Carre, J. Schultz, *J. Adhesion* **17**, 135 (1984).
9. C. A. Dahlquist, in, D. D. Eley, Ed. *Adhesion: Fundamentals and Practice*, (MacLaren, London, 1966).
10. H. W. Yang, *PSTC Annual Technical Seminar Proc.*, Schaumburg, Illinois, USA, May, 1991.
11. S. S. Voyutskii, *Autohesion and Adhesion of High Polymers* (Wiley Interscience, New York, 1963).
12. R. M. Vasenin, in D. D. Eley, Ed. *Adhesion: Fundamentals and Practice*, (MacLaren, London, 1966).
13. K. Jud, H. H. Kausch, J. G. Williams, *J. Materials Sci.* **16**, 204 (1981).
14. P.-G. de Gennes, *Physics Today* **36(6)**, 33 (1983).
15. R. P. Wool, *ACS Polym. Preprints* **23(2)**, 62 (1982).
16. P.-G. de Gennes, *J. Chem. Phys.* **55**, 572 (1971).
17. P.-G. de Gennes, Private Communications (1988 & 1992).
18. G. M. Bristow, W. F. Watson, *Trans. Faraday Soc.* **54**, 1731 (1958).
19. J. E. Mark, A. Eisenberg, W. G. Graessley, L. Mandelkern, J. L. Koenig, *Physical Properties of Polymers* (American Chemical Society, Washington, D. C., 1984), p. 134.
20. J. D. Ferry, *Viscoelastic Properties of Polymers* (John Wiley & Sons, New York, 1980), 3rd ed., p. 374.
21. *Polymer Handbook*, J. Brandrup, E. H. Immergut, Eds. (John Wiley & Sons, New York, 1989), 3rd ed., VII/1.
22. J. M. McKelvey, *Polymer Processing* (Wiley, New York, 1962), p. 202 & 363.